Single-mask fabrication of micro-probe electrode array with various tip heights and sharpness using isotropic and anisotropic etching

Young-min Shin[1], Yong-Kweon Kim[1], Seung-Ki Lee[2], Jae-Hyoung Park[2] ✉

[1]*Department of Electrical Engineering and Computer Science, Seoul National University, Seoul 151-744, Republic of Korea*
[2]*Department of Electronics and Electrical Engineering, Dankook University, Yongin 448-701, Republic of Korea*
✉ *E-mail: parkjae@dankook.ac.kr*

Published in Micro & Nano Letters; Received on 22nd March 2018; Revised on 20th April 2018; Accepted on 16th May 2018

In this work, a silicon-based micro-probe array was fabricated using multi-step deep reactive ion etching (DRIE) and reactive ion etching (RIE) processes. The micro-probe structure was implemented using a micromachining technique through a combination of two anisotropic DRIE and two isotropic RIE processes with a single etch mask. The cone-shaped tip height and tapered tip-end angle were experimentally varied with respect to the first DRIE depth. As the first DRIE depth was decreased, the micro-probe tip height increased and the sharpness consequently improved. The conductive layer was exposed only at the tip ends of the micro-probe to form a conical ultra-micro electrode, and it was characterised via cyclic voltammetry measurements.

1. Introduction: In biological applications, micro fabricated probe arrays with small size and a sharp tip have been developed, which have the advantages of reducing damage during tissue or cell penetration. The micro-probe arrays are used as electrodes for the stimulation and signal measurements with the tissue or cell penetration [1]. With the growth of micromachining technology, various micro-probe type electrodes have been demonstrated using micro fabrication methods such as glass reflow process [2], vapour liquid solid method [3], titanium needle electrodes using electrochemical etching method [4], and thermal drawing method [5]. In many studies, micro-probe structures have been developed to enhance the quality of the signal recording for biological measurements.

One of the important factors affecting signal quality is electrode chemical crosstalk. To improve the signal quality of individual electrodes, chemical crosstalk should be minimised that affects signal quality. This chemical crosstalk phenomenon is affected by the spacing between the electrodes. The electrode chemical crosstalk can be avoided when the distance between the sensing electrode and the adjacent electrode is >100 μm [6]. To minimise the chemical crosstalk, Xiao *et al.* reported biosensor using microelectrode array with 140 μm spacing, which is fabricated with bulk silicon substrate [7]. Utah electrode array (UEA) is vertical probe electrode array for brain recording and stimulation which is fabricated based on the micro fabrication technology. The UEA structures were studied to be applied to implantable biomedical devices used in neurophysiological applications [8, 9]. The spacing between electrodes ranges over hundreds of microns. Therefore, individual probe electrodes should be isolated from neighbouring electrodes to reduce crosstalk between probes and also to enhance the signal output response.

Silicon-based vertical micro-probe electrode array was implemented using the one step deep reactive ion etching (DRIE) and reactive ion etching (RIE) processes presented in the authors' previous research [10]. In the previous study, the silicon pillars patterned using a single DRIE process were sharpened through an isotropic RIE process to form a micro tip structure at the end of probe. However, the micro tips formed with pillar pitch of over 40 μm have short length and small aspect ratio because the tip shape is determined by the etch rate difference at the sidewall depending on the gap between patterns. The wide gap between pillars make the etch rate at the bottom side higher than the top, forming short micro tip with small aspect ratio. Therefore, it is difficult to fabricate a micro-probe array with large gap between electrodes to reduce crosstalk. In this Letter, a fabrication method using multi DRIE and RIE processes to realise a silicon-based sharp micro-probe electrode array with a wide pitch between the probes is presented. A single photolithography process was performed through the entire fabrication process. The cone-shaped tip height and sharpness of the tip were adjusted with respect to the proposed simple fabrication process.

2. Fabrication and analysis: The steps of the proposed fabrication process are shown in Fig. 1. A silicon wafer with the thickness of 525 μm and the diameter of 4 in. was used as the substrate for the micro-probe array.

Firstly, a 1-μm-thick SiO_2 layer was deposited using a plasma enhanced chemical vapour deposition process. This SiO_2 film is used as a hard mask in all the dry etching steps to form the micro-probe structure. Then, the AZ4330 Photoresist is uniformly coated 3 μm on the entire wafer surface by spin coating method and patterned on the SiO_2 layer by photolithography process. The SiO_2 hard mask was patterned through the oxide etch process, the vertical silicon pillar is formed using standard anisotropic DRIE in an inductively coupled plasma etcher, which defines the cone-shaped tip part of the micro-probe during the isotropic RIE process that immediately follows (Fig. 1*a*). Thus, the depth of the first silicon DRIE was varied as 50, 100, and 150 μm, respectively. The diameter of the vertical pillar is 80 μm. The vertical silicon pillar is then etched isotropically using the RIE process to form the cone-shaped tip part (Fig. 1*b*). The isotropic RIE step was conducted under the silicon etching conditions in the standard DRIE process without polymer deposition and removing steps. The applied RF power is 825 W. The gas flow rate of SF_6, C_4F_8 and Ar is 100, 0.5, and 30 sccm, respectively, with the chamber pressure of 23 mTorr. The silicon pillars were sharpened in this process due to the etch rate variation at the sidewall of the pillar. The measured etch rate of the sidewall at the tip position was ~0.1 μm/s. The first isotropic RIE process time is adjusted so that the etch mask and the top section of the silicon pillar remains on the sharpened tip part. Next, the silicon was anisotropically etched using the second DRIE process with oxide mask on top of the pillar (Fig. 1*c*). The total height of the micro-probe was determined through the second DRIE process. The conical tip height and sharpness were primarily controlled using the first DRIE and RIE processes. Therefore, a micro-probe array with wide pitch can be achieved

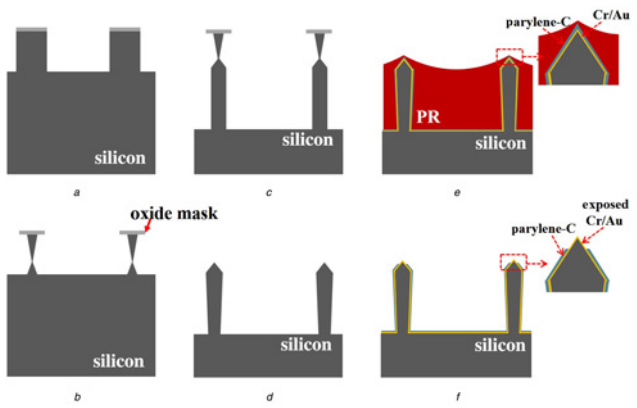

Fig. 1 *Fabrication procedure of the micro-probe electrode array*
a First DRIE process
b First RIE process
c Second DRIE process
d Second RIE process
e Cr/Au, Parylene-C coating and photoresist coating process for Parylene-C etching step
f Micro-probe electrode

without affecting the conical tip height and sharpness. The micro-probe structure was completed through the second RIE process (Fig. 1*d*). The top part on the conical silicon tip was detached from the micro-probe's body and the sharp tip end was formed after the second RIE process. To verify the electrical properties of the fabricated micro-probe, Cr/Au (100/1000 Å) was deposited as a conductive layer on the micro-probe and then 3000 Å Parylene-C was deposited as an insulation layer. The wafer was diced in 1.5 cm × 1.5 cm samples before spin coating of photoresist. Double coating of thick photoresist (AZ4620) was used to cover the Parylene-C on the micro-probe with high aspect ratio. Spin coating of photoresist was performed at 1000 rpm and the resist was baked at 110°C (Fig. 1*e*) and followed by the RIE process to remove the Parylene-C at the tip-end without additional photolithography process. The photoresist at the tip-end was very thin compared to other parts of the micro-probe after spin coating. Therefore, the photoresist at the tip-end was etched first during the RIE process, and then, the exposed Parylene-C was removed to expose the conductive layer, thus forming a cone-shaped ultra-micro electrode (UME) (Fig. 1*f*). The isotropic etch process was performed using 100 sccm O_2 and 5 sccm Ar with a power of 200 W at 100 mTorr.

Fig. 2 shows the fabricated micro-probe electrode array. The conical tip height and the sharpness could be controlled with the

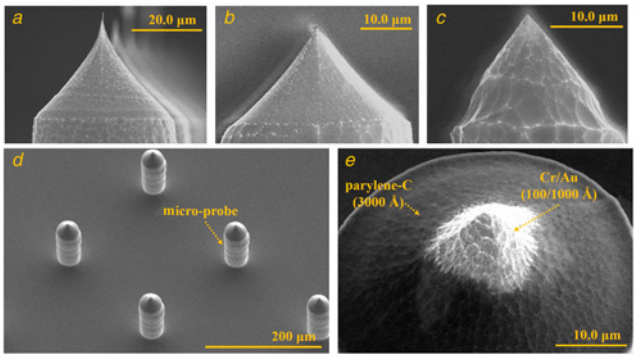

Fig. 2 *Fabrication results*
a Conical tip shape with the first DRIE depth of 50 μm
b Conical tip shape with the first DRIE depth of 100 μm
c Conical tip shape with the first DRIE depth of 150 μm
d Micro-probe array
e Exposure of electrode at the tip end

first DRIE depth as shown in Figs. 2*a*–*c*. The pitch of micro-probe is 190 μm, and Fig. 2*e* shows exposed UME at the probe tip end. Fig. 3 shows the measured conical tip height and tip-end angle increasing with the first DRIE depth. In the subsequent RIE process, the long silicon pillar structure is thermally isolated more than the short pillar and the isotropic etch rate on the sidewall becomes fast [11]. Therefore, the height of the conical tip decreases with increasing depth of the first DRIE process as shown in the measurement results. The tapered tip-end angle denoted by the inset in Fig. 3 was measured at 13°, 28° and 34°, with first DRIE depth of 50, 100 and 150 μm, respectively, which shows that the sharpness could also be controlled via the first DRIE depth. It is known that when the micro-probe is used for the biological applications, the small tapered tip-end angle induces small insertion force and minimum tissue damage [12].

3. Cyclic voltammetry (CV) measurement: The fabricated micro-probe with a conical UME was characterised via CV measurements. The CV measurement was carried out using a solution of $K_4Fe[(CN)_6]$ and a supporting electrolyte of KCL in a three-electrode setup. The fabricated micro-probe UME was used as a working electrode, while a Pt wire and Ag/AgCl electrode were used as a counter and a reference electrode, respectively. The current was recorded at 50 mV/s scan rate within a voltage range of −0.7 to 0.7 V.

The measurement results are shown in Fig. 4. The CV results exhibit the typical behaviour of UMEs and it can be seen that the measured current increases proportionally with the concentration of $K_4Fe[(CN)_6]$. In order to analyse the CV results, the steady-state limiting current of the exposed conductive layer at the tip-end was

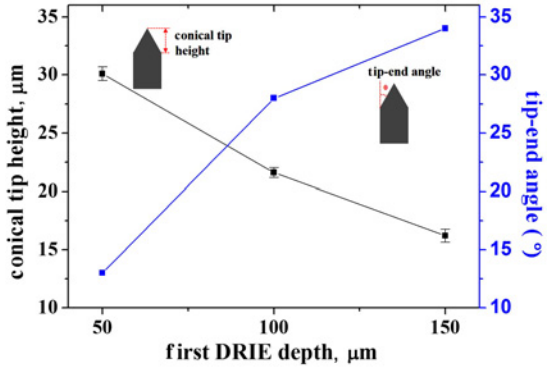

Fig. 3 *Measured conical tip height and probe-end angle with increasing first DRIE depth*

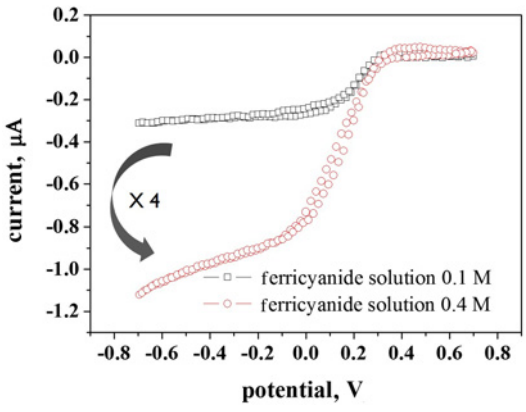

Fig. 4 *CV measurement results using the fabricated micro-probe electrode array with different ferricyanide concentrations*

doi: 10.1049/mnl.2018.5064

Table 1 Parameters used in the calculation of the steady-state limiting current

Parameters	Value	Unit
faraday constant (F)	9.65×10^4	C mol^{-1}
diffusion coefficient (D)	7.00×10^{-6}	cm^2 s^{-1}
bulk concentration (c^b)	100, 400	mM
aspect ratio (H)	1.06	—
radius of the insulation sheath (R_g)	1.04	—

Table 2 Comparisons of measured currents with estimated values

Concentration of $K_4Fe[(CN)_6]$, M	Current		
	Estimated value, nA	Measured value, nA	Error, %
0.1	311	312	0.3
0.4	1244	1113	11

theoretically calculated and compared with experimental data. For the theoretical calculation of the steady-state limiting current, the analysis was conducted using the theory applicable to most of the conical micro electrodes studied by Leonhardt *et al*. [13]. Leonhardt *et al.* report that the steady-state limiting current varies with insulation angle and insulation thickness. The reason why the steady-state limiting current changes is that if the insulation thickness has small values, the amount of back diffusion around the insulation coating can be controlled according to the insulation angle, so that the value of the steady-state limiting current can be changed. Since the micro-probe structure fabricated in this Letter also uses a thin film of 3000 Å Parylene-C as the insulation layer, it can be analysed with Leonhardt's results. The following equations are applicable to obtain the steady-state limiting current:

$$i_{\text{tip}} = nFDc^{\text{b}}r_{\text{tip}}\left[A_H + B_H\left(R_g + C_H\right)^{-D_H}\right] \quad (1)$$

where n is the number of electrons transferred during the reaction, F is the Faraday constant, and D is the diffusion coefficient of $K_4Fe[(CN)_6]$. c^{b} is the bulk concentration, and r_{tip} is the diameter of the cone of the fabricated micro-probe. R_g is the radius of the insulation sheath, which is the ratio of the insulation layer thickness to the radius of the micro-probe

$$A_H = 1.47972H + 3.69141 \quad (2)$$

$$B_H = 0.12629H^2 + 0.65894H - 0.01259 \quad (3)$$

$$C_H = 0.0115H^2 + 0.25251H - 0.72687 \quad (4)$$

$$D_H = -0.00943H^2 + 0.08213H + 0.83038 \quad (5)$$

Other parameters are determined by the H value, which is the aspect ratio of the conical tip. Table 1 summarises the variables used to calculate the theoretical values. As can be observed in Table 2, the measured results are in good agreement with the estimated values.

4. Conclusion: In this Letter, a fabrication method for a micro-probe array with conical sharp tips at the end using multi-step DRIE and RIE with a single photolithography process has been presented. The first DRIE depth control can adjust the conical tip height and tapered tip-end angle, and the overall height of the micro-probe electrode was determined using the second DRIE process. Therefore, a micro-probe electrode array with wide pitch can be obtained using a sharp conical tip end. Moreover, the electrochemical characteristics of the fabricated micro-probe electrode were tested and verified through CV measurements.

5. Acknowledgment: This research was supported by Basic Science Research Program through the National Research Foundation of Korea (NRF) funded by the Ministry of Science and ICT (grant no. NRF2016R1A2B4008059)

6 References

[1] Patil A.C., Thakor N.V.: 'Implantable neurotechnologies: a review of micro- and nanoelectrodes neural recording', *Med. Biol. Eng. Comput.*, 2016, **54**, (1), pp. 23–44

[2] Lee Y.T., Lin C.W., Lin C.M., *ET AL.*: 'A pseudo 3D glass microprobe array: glass microprobe with embedded silicon for alignment and electrical interconnection during assembly', *J. Micromech. Microeng.*, 2010, **20**, (2), p. 025014

[3] Kawano T., Harimoto T., Ishihara A., *ET AL.*: 'Electrical interfacing between neurons and electronics via vertically integrated sub-4 μm-diameter silicon probe arrays fabricated by vapor-liquid-solid growth', *Biosens. Bioelectron.*, 2010, **25**, (7), pp. 1809–1815

[4] Kitamura N., Chim J., Miki N.: 'Electrotactile display using micro-fabricated micro-needle array', *J. Micromech. Microeng.*, 2015, **25**, (2), p. 025016

[5] Ren L., Jiang Q., Chen K., *ET AL.*: 'Fabrication of a micro-needle array electrode by thermal drawing for bio-signals monitoring', *Seonsors*, 2016, **16**, p. 908

[6] Yu P., Wilson G. S.: 'An independently addressable microbiosensor array: what are the limits of sensing element density?', *Faraday Discuss.*, 2000, **116**, pp. 305–317

[7] Xiao G., Song Y., Zhang S., *ET AL.*: 'A high-sensitive nano-modified biosensor for dynamic monitoring of glutamate and neural spike co-variation from rat cortex to hippocampal sub-regions', *J. Neurosci. Methods*, 2017, **291**, pp. 122–130

[8] Sharma A., Rieth L., Tathireddy P., *ET AL.*: 'Evaluation of the packaging and encapsulation reliability in fully integrated, fully wireless 100 channel Utah slant electrode array (USEA): implications for long term functionality', *Sens. Actuators A: Phys.*, 2012, **188**, pp. 167–172

[9] Wark H., Sharma R., Mathews K., *ET AL.*: 'A new high-density (25 electrodes/mm2) penetrating microelectrode array for recording and stimulating sub-millimeter neuroanatomical structures', *J. Neural Eng.*, 2013, **10**, p. 045003

[10] Ha J.G., Lee S.K., Bai S.J., *ET AL.*: 'Conductive microtip electrode array with variable aspect ratio using combination process of reactive ion etching', *J. Micromech. Microeng.*, 2013, **23**, (11), p. 115009

[11] Lee Y.S., Jang Y.H., Kim Y.K., *ET AL.*: 'Thermal de-isolation of silicon microstructure in a plasma etching environment', *J. Micromech. Microeng.*, 2013, **23**, (2), p. 025026

[12] Ma G., Wu C.: 'Microneedle, bio-microneedle and bio-inspired microneedle: A review', *J. Control. Release*, 2017, **251**, pp. 11–23

[13] Leonhardt K., Avdic A., Lugstein A., *ET AL.*: 'Atomic force microscopy-scanning electrochemical microscopy: influence of tip geometry and insulation defects on diffusion controlled currents at conical electrodes', *Anal. Chem.*, 2011, **83**, (3), pp. 2971–2977